



# Gold-thiolate cluster emission from SAMs under keV ion bombardment: Experiments and molecular dynamics simulations

B. Arezki<sup>a,\*</sup>, A. Delcorte<sup>a</sup>, A.C. Chami<sup>b</sup>, B.J. Garrison<sup>c</sup>, P. Bertrand<sup>a</sup>

<sup>a</sup> *Université Catholique de Louvain PCPM, Croix du Sud, 1-B-1348 Louvain-la-Neuve, Belgium*

<sup>b</sup> *Laboratoire Interactions Rayonnement-Matière, BP 32 El Alia, USTHB Bab Ezzouar, Algiers, Algeria*

<sup>c</sup> *Department of Chemistry, 152 Davey Laboratory, The Pennsylvania State University, University Park, PA 16802, USA*

## Abstract

In this contribution the emission of gold-molecule cluster ions from self-assembled monolayers (SAMs) of alkanethiols on gold is investigated using time-of-flight secondary ion mass spectrometry (ToF-SIMS). Layers of alkanethiols  $[\text{CH}_3(\text{CH}_2)_n\text{SH}]$  with various chain lengths ( $n = 8, 12, 16$ ) have been chosen because they form well-ordered molecular monolayers on gold. First, we compare and interpret the yields and energy spectra of gold-thiolate cluster ions, obtained for different thiol sizes. Our results show that the unimolecular dissociation of larger aggregates in the acceleration section of the spectrometer constitutes a significant formation channel for gold-molecule clusters. Second, we present preliminary results of molecular dynamics simulations performed in order to improve our understanding of the cluster emission processes. These calculations have been conducted using 8 keV projectiles and a long-range term in the hydrocarbon potential in order to account for the van der Waals forces between the thiol chains.

© 2003 Elsevier B.V. All rights reserved.

## 1. Introduction

To improve our understanding of cluster sputtering from adsorbed organic layers, we have chosen to investigate self-assembled monolayers (SAMs) of alkanethiols on gold under 15 keV  $\text{Ga}^+$  bombardment. These assemblies have been intensively characterized in the last decade by a variety of complementary analytical techniques [1]. The alkanethiol molecules chemisorb spontaneously on

gold, as (M–H) thiolates (M being the whole alkanethiol molecule), via a strong and covalent interaction between the sulfur headgroup and the surface atoms, forming a two-dimensional crystal lattice on the underlying substrate with a tilt angle of about  $30^\circ$  from the surface normal [2]. The alkyl chains are densely packed and highly stable owing to van der Waals forces. They form a well-defined and ordered structure that constitutes an ideal model system to study the complex phenomena governing molecular desorption from organic surfaces upon energetic ion bombardment. Static secondary ion mass spectrometry (s-SIMS) has proved to be a powerful tool to probe the surface chemistry of SAMs and to study fundamental

\* Corresponding author. Tel.: +32-104-73583; fax: +32-104-73452.

E-mail address: [arezki@pcpm.ucl.ac.be](mailto:arezki@pcpm.ucl.ac.be) (B. Arezki).

processes leading to molecular sputtering from these assemblies [3–8]. However, only a few studies have been carried out concerning the origin of the gold-thiolate cluster ions observed in the SIMS mass spectra.

In their pioneer work studying SAMs by SIMS, Tarlov et al. [3] suggested that, considering the 3-fold hollow adsorption sites of the thiolate head groups, the  $(M-H)_2Au^-$  ion cluster can not eject intact but it probably results from a recombination reaction after escaping the surface. On the grounds of molecular dynamic simulations, Liu et al. [6] proposed that the alkanethiolate eject intact from the surface and then recombine with a gold atom to form a precursor  $Au(M-H)$  cluster before undergoing further recombination processes to form larger gold-thiolate clusters. Recently, Wolf et al. [7] have suggested different mechanisms inspired from the same precursor cluster concept. In our previous work, the kinetic energy distributions (KEDs) of gold-thiolate cluster ions, measured using ToF-SIMS, showed that collisional effects are responsible for their emission [8].

In this contribution we focus on the metastable decay reactions of excited gold-thiolate cluster ions during their flight to the detector. We investigate methyl-terminated alkanethiols  $CH_3(CH_2)_n SH$  with various chain lengths ( $n = 8, 12, 16$ ). To explain the mechanisms of cluster emission, molecular dynamic (MD) simulations have been performed using 8 keV projectiles and a long-range term in the hydrocarbon potential. In this manner, van der Waals forces between the alkyl chains are taken into account.

## 2. Material and methods

### 2.1. Sample preparation

The studied alkanethiols were octanethiol (C8) (>98%, Aldrich), dodecanethiol (C12) (>97%, Fluka) and hexadecanethiol (C16) (95%, Fluka) with  $n = 8, 12$  and  $16$ , respectively. The SAMs were prepared on gold films evaporated onto silicon substrates. The metallization was carried out in an Edwards evaporator. The Si wafers, cleaned with isopropanol, were first primed with a 5 nm

adhesive layer of Titanium (0.1 nm/s at  $\sim 10^{-6}$  mbar), a 100 nm Au layer was then deposited in the same conditions. The Au/Ti/Si surfaces were immediately immersed in 1 mM fresh solution prepared with the alkanethiol diluted in absolute ethanol. After immersion during  $\sim 24$  h, the samples were thoroughly rinsed in absolute ethanol, dried with a stream of  $N_2$  gas and directly transferred into the vacuum system for SIMS analysis.

### 2.2. Kinetic energy distribution (KED) measurements

The experimental setup and the KED measurement procedure have been already described in detail elsewhere [9,10]. Briefly, the KEDs were obtained in a PHI-EVANS time-of-flight microscope microprobe using a (8 kHz) pulsed  $^{69}Ga^+$  beam (15 keV; 550 pA DC current; 2 ns pulse width) [11]. The primary ion beam was focused (0.2  $\mu m$ ) and rastered onto a (120  $\mu m \times 120 \mu m$ ) area. The secondary ions, accelerated by a (3 kV) potential applied on the sample are post-accelerated (7 kV) before reaching the detector. The different energy windows are selected owing to a slit (1.5 eV passband) placed at the cross over of the secondary ion path. With this procedure, about 40 mass spectra were recorded in the mass range 0–2000 amu during 300 s acquisition time ( $1.3 \times 10^{12}$  ions/cm<sup>2</sup> per spectrum). During these experiments, a fresh area was bombarded for each energy, to avoid degradation effects.

### 2.3. MD simulations

MD computer simulation has been described extensively elsewhere [6]. This procedure consists of integrating Hamilton's equations of motion in order to obtain the positions and velocities of all the atoms in the system, as a function of time. In our study, we have modeled the 8 keV Ar bombardment of SAMs of octanethiol on Au(111). For this high-energy bombardment, we designed a larger adsorbate/Au system than that used by Liu et al. in [6]. The gold substrate is a finite microcrystallite containing 8736 Au atoms in 12 layers of 728 atoms each. The calculations are initialized by placing a total of 192 thiols on the 3-fold sites

of the Au(1 1 1) substrate in a  $(\sqrt{3} \times \sqrt{3})R30^\circ$  arrangement. Prior to Ar atom impact, the entire system is relaxed to a minimum energy configuration using periodic boundary conditions. The Ar atoms are directed along the normal to the surface. At the end of the trajectories, the ejected clusters are identified after evaluating the total internal energy of the group of linked pairs of atoms constituting this molecule. If this energy is less than zero, the group of atoms is counted as an ejected cluster.

A set of empirical pairwise and many-body potentials are used to describe the interactions between the different atoms in the system [8]. Briefly, a purely repulsive Molière potential is used for interactions with the Ar atom. The molecular dynamics/Monte Carlo corrected effective medium (MD/MC-CEM) potential is used to describe the Au–Au interactions. The S–S and S–C interactions are described by Morse potential, whereas Lennard–Jones potentials are used for S–H, Au–C and Au–H interactions. The adaptive intermolecular potential, AIREBO developed by Stuart et al. [12] is used for the hydrocarbons. This potential introduces a long-range part within the original REBO potential [13], accounting for van der Waals interactions between the thiol chains. For the particular case of the Au–S bond, a modified Morse potential is used to better describe the Au–thiolate clusters. In this potential, the energy parameter of the conventional Morse potential  $D_e$  varies as a function of the height of the Au–S pair above the surface [8].

### 3. Results and discussion

#### 3.1. Mass spectra

In the experimental study, we focus on the negative mass spectra because they exhibit a large number of molecular and gold-molecule cluster ions. Fig. 1 shows the high-mass regions of the mass spectra of the three investigated thiols. It is worthwhile mentioning that the low-mass region, up to 100 amu, is similar for all the alkanethiols, with essentially small fragments that are  $\text{CH}^-$ ,  $\text{C}_2\text{H}^-$ ,  $\text{S}^-$  and  $\text{SH}^-$ . At higher mass we observe,

for all the spectra, a variety of gold-thiolate cluster ions. These clusters are  $(\text{M-H})_2\text{Au}^-$ ,  $(\text{M-H})\text{Au}_2^-$ ,  $(\text{M-H})_2\text{Au}_3^-$ ,  $(\text{M-H})_3\text{Au}_2^-$  and  $(\text{M-H})_4\text{Au}_3^-$ . The  $(\text{M-H})^-$  thiolate ions are also observed but with less intensity.

Table 1 lists the yields of the sputtered gold-thiolate clusters and those of the substrate ion for the three thiols. First, the yields of all the gold-thiolate cluster ions decrease as a function of the thiol chain length. Second, the yields of  $(\text{M-H})_x\text{Au}_{x-1}^-$  clusters decrease more rapidly than those of  $(\text{M-H})_{x-1}\text{Au}_x^-$  clusters. Therefore, the  $(\text{M-H})_2\text{Au}^-$  is the prominent peak for C8 and C12 SAMs, whereas for C16, the most intense peak is  $(\text{M-H})\text{Au}_2^-$ . Overall, the intensity decrease of  $\text{MAu}^-$  and  $(\text{M-H})^-$  with increasing chain length is very slow as compared to all the other clusters. Finally, the Au-signal increases when the chains become longer.

The trend of decreasing intensity with increasing chain length is in agreement with the literature [3,4,7]. It was explained by the reduction of the secondary ion survival probability when the ejected clusters are heavier [3] and by the stronger intermolecular interactions between the hydrocarbon chains as  $n$  increases [7]. In addition, simply increasing the size of molecular species has been shown to reduce their yield [14], because fragmentation processes become predominant. The slower decay of  $(\text{M-H})_{x-1}\text{Au}_x^-$  cluster ions has also been observed but there is no explanation for this trend yet. The behavior of increasing  $\text{Au}^-$  signal has been noticed by Tarlov et al. [3]. A similar feature has been reported by Bolbach et al. when studying secondary ion emission from Langmuir–Blodgett films up to 50 Å of thickness [15]. This effect can be explained by the change in ionization probability induced by the presence of the organic matrix, which masks the attenuation of the signal, predominant beyond two-monolayer coverage.

#### 3.2. Kinetic energy distributions

Fig. 2 compares the KEDs of the  $(\text{M-H})_x\text{Au}_{x-1}^-$  cluster ions emitted from the three investigated SAMs. The emphasis is placed on the negative part of the KEDs, where a significant yield of ejected clusters is observed. The production of clusters

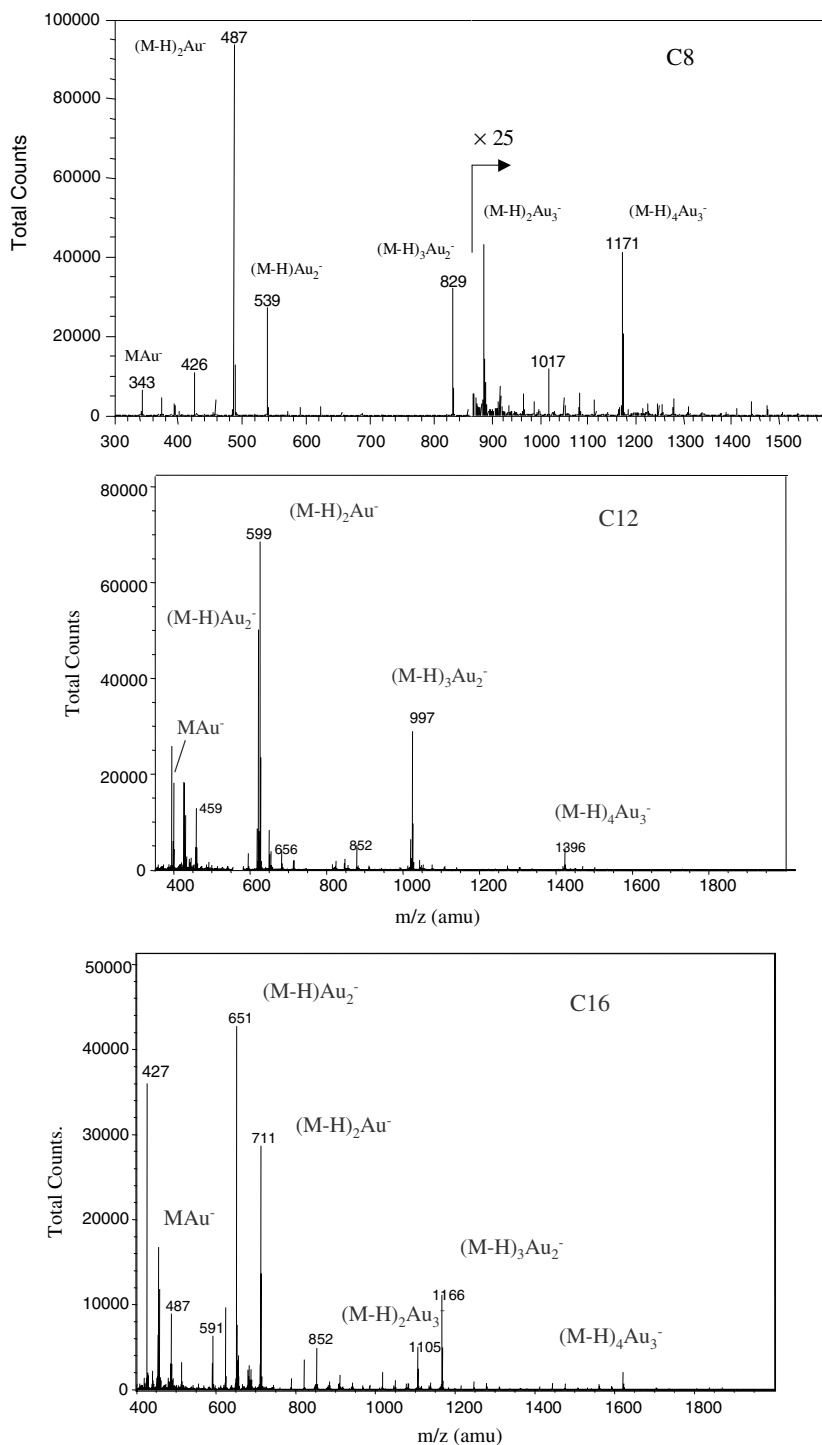


Fig. 1. Negative ToF-SIMS spectra of C8 (a), C12 (b) and C16 (c) SAMs on gold under 15 keV  $\text{Ga}^+$  bombardment.

Table 1  
Secondary ion yields of gold and gold-thiolate cluster ions emitted from C8, C12 and C16 SAMs on gold under 15 keV Ga<sup>+</sup> bombardment

Au-thiolate cluster ions	SI yield (10 <sup>-6</sup> )		
	C8	C12	C16
Au <sup>-</sup>	1180	1780	1930
(M-H) <sup>-</sup>	52	38	22
MAu <sup>-</sup>	215	200	133
(M-H)Au <sub>2</sub> <sup>-</sup>	1050	906	466
(M-H) <sub>2</sub> Au <sup>-</sup>	2090	1230	369
(M-H) <sub>2</sub> Au <sub>3</sub> <sup>-</sup>	161	155	64
(M-H) <sub>3</sub> Au <sub>2</sub> <sup>-</sup>	1190	603	131
(M-H) <sub>4</sub> Au <sub>3</sub> <sup>-</sup>	165	109	22

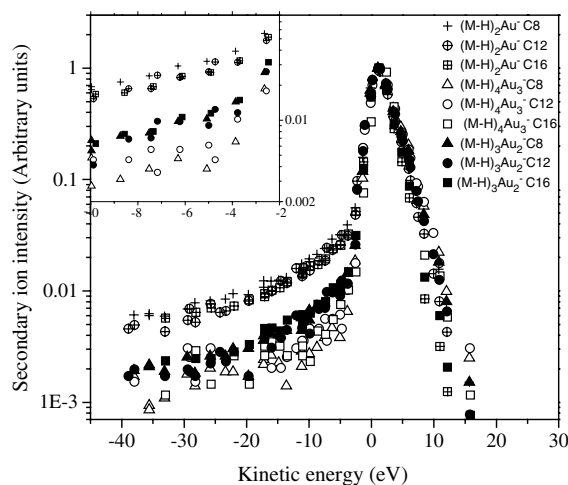


Fig. 2. Energy distributions of (M-H)<sub>x</sub>Au<sub>x-1</sub><sup>-</sup> cluster ions emitted from SAMs of C8, C12 and C16 under 15 KeV Ga<sup>+</sup> bombardment.

with an energy deficit indicates that unimolecular dissociation occurring in the acceleration of the spectrometer is an important formation process for gold-thiolate cluster ions [16]. Regardless of the chain length, the intensity corresponding to the negative energy tails in the KEDs (blown up in the inset in Fig. 2) increases with decreasing cluster size from (M-H)<sub>4</sub>Au<sub>3</sub><sup>-</sup> to (M-H)<sub>2</sub>Au<sup>-</sup>. This result suggests a scenario in which a relatively large population of high-mass aggregates is sputtered from the surface with an internal en-

ergy excess. They subsequently decompose in the vacuum, producing an important number of smaller clusters.

The second observation in Fig. 2 is that there is no effect of the thiol chain length on the KEDs of (M-H)<sub>x</sub>Au<sub>x-1</sub><sup>-</sup> ions. Indeed, the distributions of (M-H)<sub>x</sub>Au<sub>x-1</sub><sup>-</sup> ions emitted from all the three thiols merge for a given value of *x*. Therefore, the thiol size does not influence the formation process of the clusters belonging to this family. The independence of the dissociation probability on the chain length also indicates that the internal energy of ejected clusters is proportional to their size for the (M-H)<sub>x</sub>Au<sub>x-1</sub><sup>-</sup> family. Indeed, this is the condition for keeping a constant dissociation probability despite the size-related increase of the energy threshold for dissociation.

### 3.3. MD simulations

To improve our understanding of the underlying processes leading to cluster desorption from SAMs, preliminary MD simulations have been performed for a layer of octanethiols on gold, using a ‘van der Waals’ part in the potential describing the intermolecular interactions and a 8 keV projectile energy. Fig. 3 displays a characteristic trajectory leading to cluster sputtering. Various Au-thiolate clusters are hovering above the surface 5.7 ps after Ar atom impact. These large clusters are ejected from the surface as a whole, in a large-scale collective process. Such a mechanism was not predominant in Liu’s simulations, either because the projectile energy was much lower (500 eV) or because van der Waals forces were absent. In this respect, it is noteworthy that high-mass clusters have been observed in the mass spectra of octanethiol/Au for 7 keV Xe<sup>+</sup> bombardment but not for 500 eV Xe<sup>+</sup> bombardment [3]. The authors themselves suggested that the ejection of bigger clusters is the consequence of the larger quantity of energy transferred to the metal [3]. In parallel, recent MD simulations have shown that the emission of intact molecules from organic overlayers on metal substrates is mainly the result of processes initiated in the substrate [17]. The pronounced energy dependence of collective processes in the substrate observed in other MD studies [18]

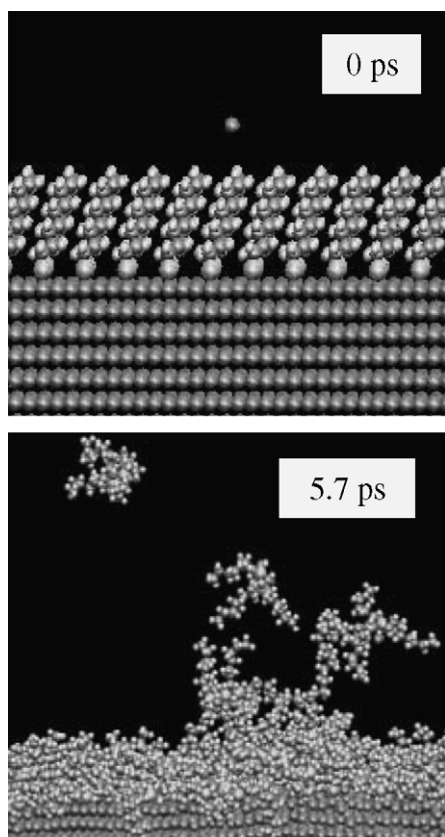


Fig. 3. Temporal snapshots of a characteristic trajectory leading to cluster sputtering from octanethiol on Au (111).

also indicates that the energy parameter is very influential. Nevertheless, at this point, the role of the van der Waals forces between the hydrocarbon chains in the dynamic processes governing the formation of these clusters can not be discarded.

Although current simulations do not allow to perform a quantitative description of the phenomena occurring far from the surface, they show that some of the emitted clusters have a sufficient internal energy to undergo metastable decay during the time scale corresponding to the experimental flight time. For example, in the trajectory depicted in Fig. 3, the internal energies calculated for  $(M-H)_3Au_2$  (29 eV) and  $(M-H)_4Au_2$  (116 eV) are higher than the value of 28 eV obtained by Delcorte et al. for the internal energy threshold for dissociation of similar-size molecule (Polystyrene tetramer) [17].

#### 4. Conclusion

The emission processes of gold-thiolate clusters from SAMs of alkanethiols of different size have been investigated by using ToF-SIMS analysis. Our kinetic energy distributions show that a significant fraction of Au-thiolate clusters is formed via the metastable decay of larger aggregates occurring in the acceleration section of the spectrometer. Therefore, another cluster formation channel has to be considered in addition to the recombination mechanisms proposed by other authors. No chain length effect has been observed in the negative part of the energy spectra of clusters belonging to the  $(M-H)_xAu_{x-1}^-$  family. The formation processes of these clusters do not depend on the thiol size.

Our preliminary MD simulations, carried out using a 8 keV projectile and including intermolecular interactions between the adsorbed thioliates, show that ejection as such is a realistic formation channel for large gold-thiolate clusters. The relatively high internal energy of these clusters indicates that they might decompose after ejection.

#### Acknowledgements

This work is supported by the PAI-IUAP P4/10 Research program on “Reduced Dimensionality Systems” of the Belgium Federal State. A.D. also acknowledges the Belgian *Fonds National pour la Recherche Scientifique* for financial support. The ToF-SIMS experiment was acquired with the support of the *Région Wallonne* and *FRFC-Loterie Nationale* of Belgium.

#### References

- [1] A. Ulman, Chem. Rev. 96 (1996) 1533.
- [2] F. Schreiber, Prog. Surf. Sci. 65 (2000) 151.
- [3] M.J. Tarlov, J.G. Newman, Langmuir 8 (1992) 1398.
- [4] D. Rading, R. Kersting, A. Benninghoven, J. Vac. Sci. Technol. A 18 (2000) 312.
- [5] Graham J. Leggett, in: J.C. Vickerman, D. Briggs (Eds.), ToF-SIMS Surface Analysis by Mass Spectrometry, IMP and Surface spectra UK, 2001, p. 573.

- [6] K.S.S. Liu, C.W. Yong, B.J. Garrison, J.C. Vickerman, *Phys. B* 103 (1999) 3195.
- [7] K.V. Wolf, D.A. Cole, S. Bernasek, *Anal. J. Phys. Chem. B* 106 (2002) 10382.
- [8] B. Arezki, A. Delcorte, P. Bertrand, *Nucl. Instr. and Meth. B* 193 (2002) 755.
- [9] P. Bertrand, L.T. Weng, *Microchim. Acta* 13 (1996) 167.
- [10] A. Delcorte, P. Bertrand, *Nucl. Instr. and Meth. B* 115 (1996) 246.
- [11] B.W. Schueler, *Microscop. Microanal. Microstruct.* 3 (1992) 119.
- [12] S.J. Stuart, A.B. Tutein, J.A. Harrison, *J. Chem. Phys.* 112 (2000) 6472.
- [13] D.W. Brenner, *Phys. Rev. B* 42 (1990) 9458.
- [14] R.S. Taylor, B. Garrison, *Chem. Phys. Lett.* 230 (1994) 495.
- [15] G. Bolbach, R. Beavis, S. Della Negra, C. Deprun, W. Ens, Y. Lebeyec, D.E. Main, B. Schueler, K.G. Standing, *Nucl. Instr. and Meth. B* 30 (1988) 74.
- [16] A. Delcorte, P. Bertrand, *Int. J. Mass Spectrom.* 184 (1999) 217.
- [17] Z. Postawa, K. Ludwing, J. Piaskowy, K. Krantzman, N. Winograd, B.J. Garrison, *Nucl. Instr. and Meth. B* 202 (2003) 168.
- [18] A. Delcorte, B.J. Garrison, *J. Phys. Chem. B* 104 (2000) 6785.